Raman Scattering in Bilayers of Saturated Phosphatidylcholines and Cholesterol. Experiment and Theory†

David A. Pink,* Trevor J. Green,‡ and Dennis Chapman

ABSTRACT: Raman spectroscopy has been applied to a model biomembrane structure in order to obtain information about the effect of cholesterol upon phospholipid hydrocarbon chain ordering. The intensity of the 1130-cm^{-1} Raman line obtained from a dipalmitoylphosphatidylcholine (DPPC) coarse aqueous dispersion was measured as a function of temperature for two concentrations, c, of cholesterol: $c = 0.15$ and $c = 0.35$. The contribution of cholesterol to this line was deduced. Intensities of all lines were taken as peak areas. By use of a theory for assigning Raman intensities to chain conformations as well as a model of lipid bilayers containing cholesterol, the temperature and concentration dependence of the 1130-cm^{-1} line was calculated. Good agreement with DPPC experimental data was obtained, and predictions are made for dimyristoylphosphatidylcholine. The experimental results are interpreted in terms of a DPPC–cholesterol phase diagram and the average number of gauche bonds per DPPC molecule.

Cholesterol is an important component of biological membranes, and many studies have been made of phospholipid–cholesterol interactions by using a range of physical techniques. It is now generally accepted that when cholesterol is dispersed with a saturated phospholipid, such as dipalmitoylphosphatidylcholine (DPPC),[1] in water in the form of lipid bilayers that below the temperature of the gel–liquid-crystal transition of the pure lipid (T_c) it has the effect of disrupting the close packing of the fatty acid hydrocarbon chains and thus "fluidizes" the bilayer, whereas above T_c it inhibits chain motion and thus "rigidifies" the lipid bilayer (Oldfield & Chapman, 1972).

The technique of Raman spectroscopy is finding increasing use for the study of phospholipid–water systems in both biological and model membranes. Lippert & Peticolas (1971) made use of the 1100-cm^{-1} region of the lipid Raman spectrum in order to monitor the effect of temperature on some lipid–water dispersions containing cholesterol, while Spiker & Levin (1976) studied the effect of cholesterol in both multilayer and single-wall vesicle assemblies. Bunow & Levin (1977) and Spiker & Levin (1975) studied the effects of cholesterol on the CH-stretching modes and the skeletal optical modes of multilayers. A recent review by Wallach et al. (1979) also surveys work done on cholesterol in systems other than saturated phospholipids. We have recently examined the 1100-cm^{-1} region of the spectrum both experimentally and theoretically in order to obtain information about chain conformations.

Because the probability of a hydrocarbon chain being in a given conformation cannot be deduced in an unequivocal way from the 1130-cm^{-1} band intensity data, we extended a theoretical model of hydrocarbon chain dynamics in a bilayer of saturated lipids (Pink & Chapman, 1979), if necessary, in the presence of a given concentration of intrinsic foreign molecules. The chain conformation probabilities obtained from the theoretical model, together with the appropriate assignment of an 1130-cm^{-1} Raman intensity to a given conformation (deduced from theories of Raman scattering from hydrocarbon chains), allowed an overall relative 1130-cm^{-1} band intensity from the lipid bilayer to be calculated. This calculated intensity was compared to the relative Raman intensity obtained experimentally as a function of temperature.

The theoretical model was shown to successfully account for the experimental Raman intensity obtained from a coarse aqueous dispersion of DPPC and also to account for previous data obtained from distearoylphosphatidylcholine by Yellin & Levin (1977a). The hydrocarbon chain conformation probabilities yielded by the model serve to characterize the system, and it was found that the average number of gauche bonds per chain was 0.5, 1.2, and 1.5 at temperatures of 0 °C, 35 °C, and just below the T_c, respectively, for DPPC. These results are in good agreement with the estimates made by Yellin & Levin (1977b), who made use of the van't Hoff enthalpy expression.

In the present paper, we examine, using Raman spectroscopy, the DPPC–cholesterol system. In this case, the Raman spectrum, in addition to lines from the lipid, contains lines due to Raman scattering from the cholesterol molecules. The theoretical model (besides taking account of molecular interactions) needs to take into account the cholesterol hydrocarbon chain contribution to the 1130-cm^{-1} Raman intensity, plus a background cholesterol intensity, together with a variation in the lipid reference line intensity (at 718 cm^{-1}), this intensity depending on the cholesterol concentration. We examine the experimental Raman intensity obtained from the system, characterizing the system again by hydrocarbon chain conformational probabilities. The interpretation of some of the data makes use of a DPPC–cholesterol phase diagram (D. A. Pink, A. Georgallas, M. J. Zuckermann, and M. O. Steinitz, unpublished calculations).

Experimental Procedures

L-β,γ-Dipalmitoyl-α-phosphatidylcholine, produced by Fluka (purissimum grade), was obtained from Fluorochem Ltd.,

† From the Theoretical Physics Institute, St. Francis Xavier University, Antigonish, Nova Scotia, Canada B2G 1C0 (D.A.P.), and the Department of Biochemistry and Chemistry, Royal Free Hospital School of Medicine, University of London, London WC1N 1BP, England (T.J.G. and D.C.). *Received December 17, 1980; revised manuscript received July 9, 1981.* This work was supported in part by the Natural Sciences and Engineering Research Council of Canada, the Science Research Council, the Wellcome Trust, and the University Council for Research, St. Francis Xavier University.

‡ Present address: Centre de Recherche Paul Pascal, Domaine Universitaire, 33405 Talence Cedex, Bordeaux, France.

[1] Abbreviations used: DMPC, dimyristoylphosphatidycholine; DPPC, dipalmitoylphosphatidylcholine; DSPC, distearoylphosphatidylcholine; TO, transverse optic.

0006-2960/81/0420-6692$01.25/0

Table I: C-M Hydrocarbon Chain State Configurations and Relative Raman Intensities

state		length (C–C bond units)	degeneracy	relative Raman intensity (C-M) C-14	C-16	C-18	internal energy
all-trans	G	$M-1$	1	14.00	16.00	18.00	0
intermediate	1	$M-2$	4	5.86	7.63	9.44	E_g[a]
	2	$M-3$	4	1.86	3.13	4.56	
	3	$M-4$	4	0.14	0.63	1.44	
	4 kink	$M-2$	$2M-12$	7.14	9.00	10.89	$2E_g$
	5	$M-3$	$2M-16$	2.57	4.00	5.56	
	6	$M-4$	$2M-20$	0.29	1.00	2.00	
	7	$M-3$	$8M-64$	1.92	3.18	4.61	$3E_g$
	8	$M-4$	$16M-160$	0.16	0.66	1.42	
melted	E	$20.4(M-1)/34.0$	$D_E(M)$	0.71	0.94	1.11	$E_E(M)$

[a] E_g is the energy required to form a gauche bond, $E_g = 0.45 \times 10^{-13}$ erg (Pink et al., 1980).

Glossop, Derbyshire. Cholesterol (Δ^5-cholesten-3-ol, Sigma grade +99%, standard for chromatography) was obtained from the Sigma London Chemical Co., Kingston-Upon-Thames, Surrey. Both were used without further purification.

Cholesterol was dissolved in 95/5 (v/v) benzene/methanol and the solution added in the required amounts to dry DPPC. The samples were lyophilized and then combined with 2.5 parts by weight of doubly distilled deionized water in 3.5-mm diameter sample tubes. Vortex mixing, performed above the lipid gel–liquid-crystal transition temperature, yielded homogeneous dispersions, which were then allowed to equilibriate. The dispersions were compacted by light centrifugation before use.

Raman spectra as functions of temperature were recorded on a Spex Ramalog 5 instrument as described previously (Pink et al., 1980). The intensities of the 1130-cm^{-1} line were measured with respect to the 718-cm^{-1} DPPC line which has been assigned to a C–N stretching mode in the head group. The temperature dependence of this line is very much less than that of the 1130-cm^{-1} line (Gaber & Peticolas, 1977; Gaber et al., 1978), and as customary, we take it to be temperature independent. These lines were decomposed from overlapping neighbors by eye, and their area ratios were obtained by weighing paper cutouts of the peaks. Each Raman intensity presented is the average intensity ratio (I_{1130}/I_{718}) from four spectra, normalized by the average intensity ratio obtained from pure DPPC–H_2O bilayers at −157 °C (1.64 ± 0.07) when the hydrocarbon chains are in the all-trans state (Pink et al., 1980). Error bars represent the estimated standard error in the mean result.

Theory

There are three aspects to consider in order to get an understanding of the dependence of the relative Raman intensity of the 1130-cm^{-1} band upon temperature and cholesterol concentration. These are (i) a model which will yield a phase diagram for a phospholipid bilayer containing cholesterol, (ii) a theory which assigns a Raman scattering intensity to each hydrocarbon chain conformer, and (iii) a way of identifying not only to what extent cholesterol contributes to the intensity of the band but also how the intensity of the reference band depends upon cholesterol concentration.

(i) A model from which the gross features of the phase diagram of a phospholipid bilayer containing cholesterol can be calculated has been constructed (D. A. Pink, A. Georgallas, M. J. Zuckermann, and M. O. Steinitz, unpublished calculations). This model is an extension of one used to study pure phospholipid bilayers (Caillé et al., 1980; Pink et al., 1980), and the phase diagrams for DPPC and DMPC for temperatures from −150 °C to above the main phase transition temperatures (T_c^{16} = 40.9 °C and T_c^{14} = 23.2 °C as calculated here, respectively) have been calculated. In this model, each site of a triangular lattice can be occupied by either a phospholipid chain in any of ten states or a cholesterol molecule. The Hamiltonian for phospholipids with $M-1$ C–C bonds per chain is

$$H = \frac{-J_0^M}{2}\Big(\sum_{\langle ij\rangle}\sum_{nm} I(n)I(m)L_{in}L_{jm} + 2\sum_{\langle il\rangle}\sum_{n} J_n I(n)L_{in}C_l + J_c\sum_{\langle lk\rangle} C_lC_k\Big) + \sum_i\sum_n\{[\Pi_0 + \rho(c)\Pi_1]A_n + E_n\}L_{in} \quad (1)$$

where L_{in} and C_l are lipid chain and cholesterol molecule projection operators for site i state n and for site l, respectively, $I(n) = (S_n/S_G)(r_G/r_n)^{5/2}$, and $S_n = \sum_p(3\cos^2\theta_{np} - 1)/2$, with p representing a summation over all C–C bonds and θ_{np} being the angle between the pth C–C bond and the local director when the chain is in state n. r_n is the effective lateral radius of a chain in state n defined as $r_n = (A_n/\pi)^{1/2}$ where A_n is the effective cross-sectional area, $A_n = A_GL_G/L_n$, and L_n is the chain length, in C–C bond units, projected onto the local director. E_n is the energy, due to trans–gauche isomerization, of a chain in state n. The states, together with their lengths for DSPC, DPPC, and dimyristoylphosphatidylcholine (DMPC), are listed in Table I. Using A_G = 20.4 Å^2, we can calculate the areas for other states. In eq 1, $\langle ij\rangle$ represents a summation over all sites and their six nearest neighbors. J_n takes on the values J_G, J_I, or J_E, depending on whether n belongs to the sets {G, 3, 5, 6, 8} ("ground"), {1, 2, 4, 7} ("intermediate"), or {E} ("excited"), and $-J_0^MJ_C$ is the interaction energy of a pair of nearest-neighbor cholesterols. $\Pi = \Pi_0 + \rho(c)\Pi_1$ is the effective lateral pressure acting in the hydrocarbon chain region due to the interactions in the polar layer which keeps the bilayer in existence (Marcelja, 1974). $\rho(c)$ is a function which depends upon the cholesterol concentration in a homogeneous phase and represents the possibility that the hydrophilic end of the cholesterol molecule may perturb the polar layer interactions and so change Π. $\rho(c)$ varies between $\rho(0) \approx 0$ and $\rho(0.5) = 1$, the latter limit being determined by the observation that not more than ~50 mol % of cholesterol can be incorporated into a phospholipid bilayer. $\rho(c)$ also increases rapidly from a small value to near its maximum value within a concentration range of ~0.1 around $c \approx 0.3$. The values of the parameters and the functional form of $\rho(c)$ are discussed by D. A. Pink, A. Georgallas, M. J. Zuckermann, and M. O. Steinitz (unpublished calculations). These values for DPPC are as follows: $J_G \simeq 0.2$, $J_I \simeq 0.9$, $J_E \simeq 0.55$, $J_c \simeq -0.75$, and $\Pi_1 \simeq -1.5$ dynes/cm. The dependence of J_0^M upon M, as well as the degeneracy and energy of the excited state E, was discussed by Caillé et al. (1980; Table II; note that the degeneracy of state 8 should be $16M-160$). As before, we chose $J_0^{16} = 0.734 \times 10^{-13}$ ergs, $E_E = 2.78 \times 10^{-13}$ ergs, $D_E = 2(3)^{11}$, and Π_0 = 30 dynes/cm.

The shortcomings of this model have been discussed by D. A. Pink, A. Georgallas, M. J. Zuckermann, and M. O. Steinitz (unpublished calculations), and it is expected to give an acceptable description of phase separation on a large scale in this system as long as structures involving a pretransition, with which this model does not concern itself, are not involved.

(ii) A theory to assign Raman scattering intensities to a given hydrocarbon chain conformer has been presented elsewhere (Pink et al., 1980). Here, we shall only summarize the results. The "1130-cm^{-1}" band which we are considering is a transverse optic (TO) mode, and the relative intensities contributed by the ten states are listed in Table I for DMPC, DPPC, and DSPC. The eight intermediate states were considered in our earlier paper but not because we found that a good fit to the Raman data was thereby obtained. Rather, they were considered a priori because (a) they had small areas close to that of the ground state (see Table I) and so could be excited relatively easily below the main transition temperature, T_c, and (b) most of them contributed nonnegligibly to the Raman intensity of the 1130-cm^{-1} band. It should also be stressed that we are concerned with a band having a half-width of a few inverse centimeters. Snyder (1967) has calculated that the corresponding TO mode of polyethylene chains with 8 or 14 carbon nuclei can shift by $\sim$1 cm^{-1} if a jog occurs in the chain. Because the width of the band which we are considering encompasses such a small shift, we shall ignore it: all TO C–C stretch chain modes with wavenumbers a few inverse centimeters around 1130 cm^{-1} will contribute to what we call the 1130-cm^{-1} band. If it becomes possible to resolve the band into sharp peaks, then the small shift in frequency brought about by one or more gauche bonds will have to be taken into account.

It has been brought to our attention that the relative Raman intensities in columns four, five, and six of Table I of our previous paper (Pink et al., 1980) have been interpreted in a way which we did not intend.[2]

It was intended that only relative Raman intensities *within a given column*, i.e., the relative Raman intensities of the different conformational states of a chain of given length, should be compared. In order to compare intensities in different columns, the listed relative intensities must be divided by M (=14, 16, or 18), which follows from the calculation of Theimer (1957). In Table I, of this paper, we have included this factor of M.

(iii) In order to estimate to what extent cholesterol contributes to the 1130-cm^{-1} band, we assumed that this contribution was proportional to the number of cholesterol molecules present. We are able to estimate a priori the contribution from the cholesterol chain by using our formula for contributions from chain conformers, and this would be temperature dependent. We were not able to identify the possible source of any other contribution, and so we assumed that it was temperature independent. In a homogeneous phase with cholesterol concentration c, the cholesterol contribution to the 1130-cm^{-1} band was thus written

$$I^{C}_{1130}(c) = Ni^{C}_{1130}(c,T)x \qquad x = c/(2 - c) \qquad (2)$$

where x is the fraction of sites occupied by cholesterol molecules, $i^{C}_{1130}(c,T)$ is the contribution by a cholesterol molecule to the absolute intensity of the 1130-cm^{-1} band, and N is the number of lattice sites.

Since we have allowed for the possibility that cholesterol can change the polar layer interaction, we must consider the possibility that the intensity of the reference band, the 718-cm^{-1} band due to C–N stretching in the head group, may depend upon the local cholesterol concentration. There is good evidence that the intensity of this band does not depend upon temperature to within the accuracy of the measurements which we report here (Bunow & Levin, 1977; Gaber & Peticolas, 1977; Gaber et al., 1978).

Recently, Bicknell-Brown & Brown (1980) have shown that the frequency and bandwidth of the 718-cm^{-1} band are insensitive to the addition of cholesterol to bilayers of DPPC at 19 °C. Accordingly, we shall consider the contribution from each DPPC molecule to the intensity of the 718-cm^{-1} band to be independent of cholesterol concentration. The intensity of the band is thus proportional only to the number of DPPC molecules present.

Thermodynamic functions are calculated in the usual way by defining a mean field Hamiltonian

$$H_0 = -\sum_i \sum_n \lambda_L(n) L_{in} - \sum_l \lambda_C C_l \qquad (3)$$

and minimizing the free energy (given by the Bogoliubov inequality, taken in the usual way as an equality) with respect to the mean fields $\lambda_L(n)$ and λ_C. The free-energy inequality is

$$F \leq F_0 + \langle H - H_0 \rangle_0 \qquad F_0 = -k_B T \ln Z_0$$
$$Z_0 = Tre^{-\beta H_0}$$
$$\langle Q \rangle_0 = TrQe^{-\beta H_0}/Z_0 \qquad \beta = 1/(k_B T) \qquad (4)$$

To obtain an expression for the relative intensity of the 1130-cm^{-1} band, we define the following: $i^{L}_{1130}(M,c,T)$ is the contribution of a single lipid chain, containing $M - 1$ CH_2 groups and one CH_3 group, to the absolute intensity of the 1130-cm^{-1} band at temperature T and cholesterol concentration c. i_{718} is the contribution from a single lipid molecule to the reference 718-cm^{-1} band, and the normalized Raman intensity is defined as

$$\frac{I_{1130}}{I_{718}} = \left[\frac{2i^{L}_{1130}(M,c,T)}{i_{718}} + \frac{2x}{1-x} \frac{i^{C}_{1130}(T)}{i_{718}} \right] \Bigg/ \frac{2i^{L}_{1130}(M,0,0)}{i_{718}} \qquad (5)$$

The intensity $i^{L}_{1130}(M,c,T)$ is obtained by calculating the thermal average by using columns four to six of Table I. The $2i^{L}_{1130}(M,c,T)/i_{718}$ ratio is obtained by dividing this result by M and multiplying it by the measured intensity ratio of the 1130-cm^{-1} band to the 718-cm^{-1} band at a sufficiently low temperature for $c = 0$. Note that when $c = 0$, $I_{1130}/I_{718} \rightarrow 1$ for all M, according to our definition. Calculations presented here for different chain lengths must be weighted by their respective chain lengths before they can be compared.

Results and Discussion

Figures 1–3 show typical spectra of pure DPPC, solid cholesterol, and a 1:1 ($c = 0.5$) mixture of DPPC and cholesterol.

We attempted to calculate $i^{C}_{1130}(T)/i_{718}$ by measuring the intensity of a band at 1672 cm^{-1}, which is apparently due only to the cholesterol. A sample of solid cholesterol was used to measure the ratio $I_{1672}(1)/I^{C}_{1130}(1,T) = i_{1672}/i^{C}_{1130}(T)$. Ratios of the intensities of the 1672-cm^{-1} band and the reference 718-cm^{-1} band were measured for cholesterol concentrations of $c = 0.15$, 0.35, and 0.5, at temperatures ranging from −61 to 22 °C. This ratio gave us $I_{1672}(c)/I_{718}(c) = 2xi_{1672}/[(1 - x)i_{718}]$, from which the required ratio of $i^{C}_{1130}(T)/i_{718}$ could be calculated. Due to difficulties in separating overlapping bands,

[2] We are grateful to M. J. Zuckermann for passing on this comment to us.

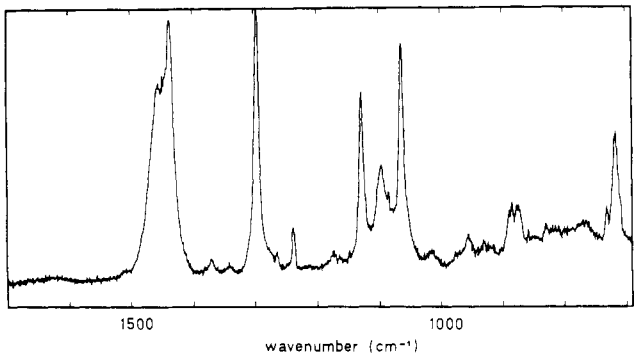

FIGURE 1: Raman spectrum of a DPPC dispersion in excess water (1:3 w/w) at 23.8 °C.

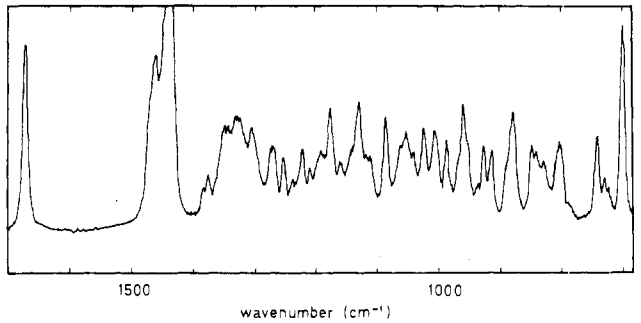

FIGURE 2: Raman spectrum of solid cholesterol at 23.3 °C.

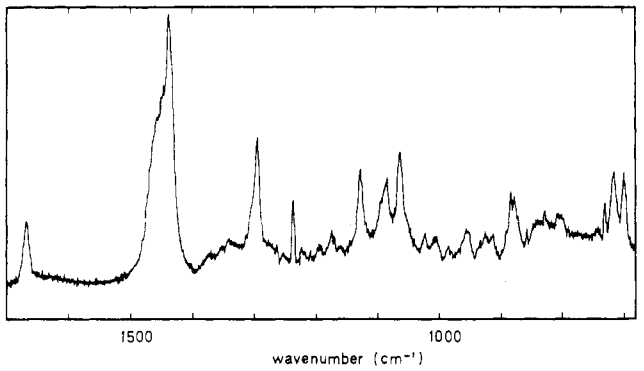

FIGURE 3: Raman spectrum of a dispersion of DPPC and cholesterol with $c = 0.5$ (1:1 mixture) at 22.0 °C.

a considerable spread of values was obtained, ranging from ~0.75 to ~1.05 (with larger values being more plausible), and we considered the average obtained in this way to be unreliable.

Accordingly, we decided to deduce the temperature-independent contribution (see remarks before eq 2) to $i^C_{1130}(T)/i_{718}$ by fitting the calculated normalized intensity to the measured value at the lowest temperature used (−162 °C) for the case of $c = 0.15$ (Figure 4). In this way, we found that

$$i^C_{1130}(T)/i_{718} = 0.975 + \text{temperature-dependent contribution} \quad (6)$$

The temperature-dependent contribution can be estimated and is less than ~0.028 so that the deduced value of $i^C_{1130}(T)/i_{718}$ lies within the range of the measured values.

We measured the value of $2i^L_{1130}(16,0,0)/i_{718}$ to be 1.64 ± 0.07 [the temperature used was −157 °C (Pink et al., 1980)]. Because the value of i^L_{1130} is proportional to the chain length, we can deduce that $2i^L_{1130}(14,0,0)/i_{718} \simeq 1.44$.

There are no free parameters to adjust in the expressions of eq 5, having obtained a number for the contribution by cholesterol to $I_{1130}(c)$. The intensities for $c = 0.15$ and $c = 0.35$ were calculated for temperatures ranging from −150 to 100 °C, and the results together with the measured intensities are shown in Figures 4 and 5. The agreement with the measured intensities is seen to be good.

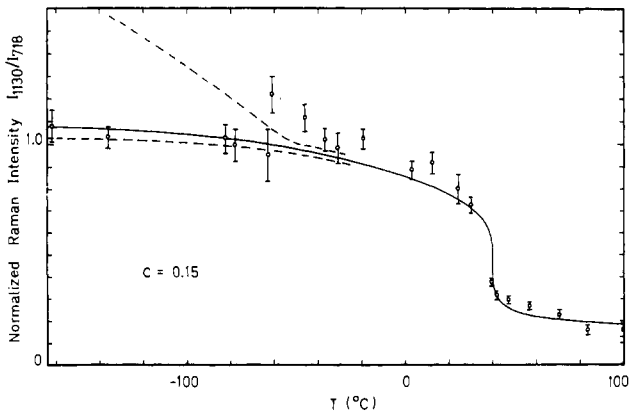

FIGURE 4: Normalized Raman intensity, I_{1130}/I_{718}, as a function of temperature for DPPC bilayers with cholesterol, $c = 0.15$. Points with error bars are measured intensities, and the solid line is the calculated intensity. The dashed lines show the normalized intensities if all the intensity were due to either of the two phases shown in Figure 6. Lower dashed line is due to the lipid-rich phase while the upper line is due to the cholesterol-rich phase.

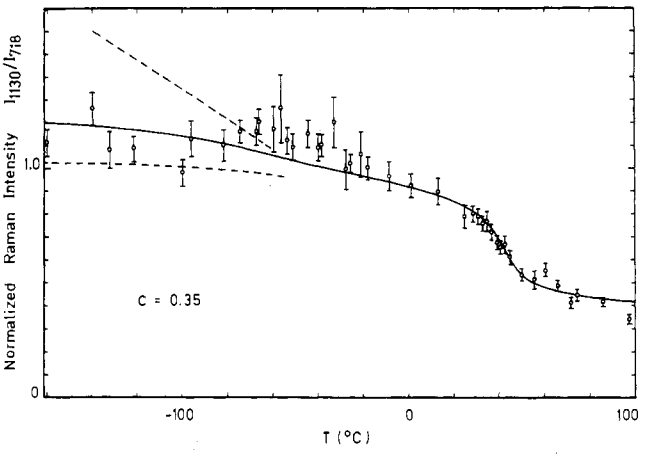

FIGURE 5: Normalized Raman intensity, I_{1130}/I_{718}, as a function of temperature for DPPC bilayers with cholesterol, $c = 0.35$. Points with error bars are measured intensities, and the solid line is the calculated intensity. The dashed lines show the normalized intensities if all the intensity were due to either of the two phases shown in Figure 6. Lower dashed line is due to the lipid-rich phase while the upper line is due to the cholesterol-rich phase.

In both cases, it can be seen that fluctuations in the measured values increase greatly as the temperature drops to ~−50 °C, and although below −100 °C the intensities for $c = 0.15$ seem to lie on a smooth curve, those for $c = 0.35$ exhibit considerable fluctuations as the temperature decreases to −150 °C. This is to be constrasted to the case of pure DPPC (Pink et al., 1980, Figure 5), where a smooth curve is obtained for all temperatures below $T \approx 25$ °C. A possible explanation of these fluctuations lies in the shape of the phase diagram obtained by Pink et al. (unpublished calculations) and reproduced here in Figure 6. The dashed lines identify $c = 0.15$ and $c = 0.35$.

It must be remembered that all calculations performed here make use of equilibrium statistical mechanics. Averages in statistical mechanics involve equating time averages with ensemble averages, and when equilibrium is established in a sufficiently short time, then averages calculated from equilibrium statistical mechanics will provide a good description of time averages. If equilibrium is not established on a time scale short compared to that of the experiment, or if some

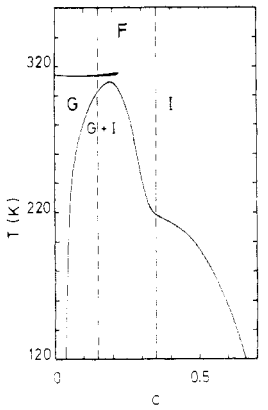

FIGURE 6: Calculated phase diagram of DPPC bilayers and cholesterol. The calculation here does not allow for the possibility of a vertical phase boundary at $c \approx 0.5$ to the right of which cholesterol precipitates out. The vertical dashed lines indicate the two concentrations studied. G, I, and F denote "gellike", "intermediate", and "fluid" phases, respectively.

aspect of the experiment inhibits the achieving of equilibrium, then calculations using equilibrium statistical mechanics can differ from results measured. It will be noticed from Figure 6 that a considerable change in phase is predicted to occur at ~−60 °C. For $c = 0.15$, phase separation occurs at ~30 °C, and the amount of the lipid-rich phase decreases until at ~−60 °C it shows an increase. For $c = 0.35$, the changes are very much more drastic. For all temperatures down to ~−50 °C, DPPC and cholesterol form a single homogeneous phase. At −50 °C, however, a drastic phase separation sets in, in which a lipid-rich phase (~5 mol % cholesterol) and a cholesterol-rich phase coexist. Such a phase separation might take a long time to come to equilibrium, because lateral diffusion in a relatively rigid bilayer at −50 °C might be very slow. It is thus possible that the measurements have sampled regions of the bilayer which are not in thermodynamic equilibrium so that greatly differing intensities might be observed. Another possibility which could lead to the establishment of an equilibrium not reflected in the calculation is the attributes of the cavity. It may be possible that phases with very different lipid concentrations (these are set up only below ~−50 °C) prefer to migrate to certain positions in the cavity, so that the laser beam would sample phases which do not reflect the equilibrium situation calculated. In Figures 4 and 5, we have considered the first possibility and calculated the intensities to be expected if only one phase was being sampled. These intensities are shown as dashed lines, the lower ones corresponding to the lipid-rich phase and the higher ones to the other phase.

Figure 7 shows the probabilities for a chain to exist in the all-trans state (G), any state with a jog on the last two C–C bonds which connect CH_2 groups on a chain (2), any state with a kink (K), or the excited "melted" state (E). These probabilities are averaged over the two phases when phase separation occurs and should be compared to the probabilities for pure DPPC shown in Figure 5 of Pink et al. (1980). One of the noteworthy features is that for $c = 0.35$ the kink state K is the most probable state for temperatures between ~−30 and ~40 °C. We see in these figures the justification for referring to the region of the phase diagram to the right of the immiscibility curve (Figure 4) as an "intermediate" region, and it is so labeled.

Figure 8 shows the average number of gauche bonds per DPPC molecule for the two concentrations and the range of temperatures considered here. The long dashes show the average number of gauche bonds per molecule in each of the two phases, and the solid line is the average number of gauche

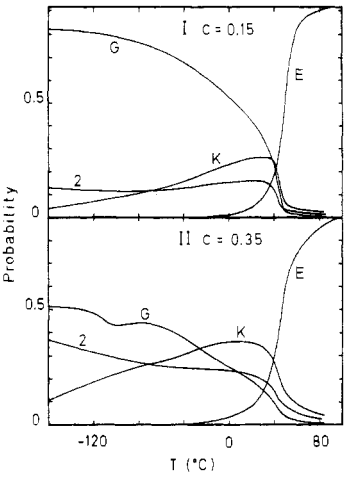

FIGURE 7: Probabilities for a hydrocarbon chain to be in four of the ten states used as a function of temperature, for DPPC. I, $c = 0.15$; II, $c = 0.35$. Calculated curves are for the all-trans ground state (G), any state with a gauche bond between carbons 14 and 15 (2), any kink state (K), or the excited melted state (E).

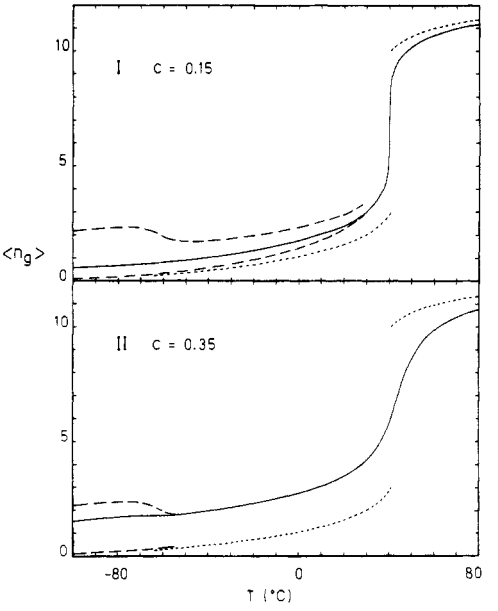

FIGURE 8: Calculated average number of gauche bonds per DPPC molecule, $\langle n_g \rangle$, as a function of temperature. I, $c = 0.15$; II, $c = 0.35$. Short dashed curves are for $c = 0$ (Pink et al., 1980), and the discontinuity shows the first-order phase transition ($T_c = 40.9$ °C). Long dashed curves are for each of the two phases shown in Figure 6, the lower curve being for the lipid-rich phase with the upper curve for the cholesterol-rich phase. The solid curve shows the average number of gauche bonds.

bonds per molecule averaged over the two phases. In the absence of rapid exchange between the two phases, the dashed lines would more properly represent the physical situation. The short dashes represent the average number of gauche bonds per DPPC molecule for pure DPPC bilayers [Figure 7 of Pink et al. (1980)]. We see that for $c = 0.15$, which is near the maximum cholesterol concentration at which a narrow specific heat peak is observed [Estep et al., 1978; Mabrey et al., 1978; Figure 4 of D. A. Pink, A. Georgallas, M. J. Zuckermann, and M. O. Steinitz (unpublished calculations)], the gellike phase is somewhat more disordered, and the fluidlike phase is somewhat less disordered, than a pure DPPC bilayer at the same temperature. It is only for temperature near the specific heat peak that DPPC molecules have one or two gauche bonds more ($T < T_c$) or less ($T > T_c$) in the presence of cholesterol than DPPC molecules for $c = 0$. This is another justification

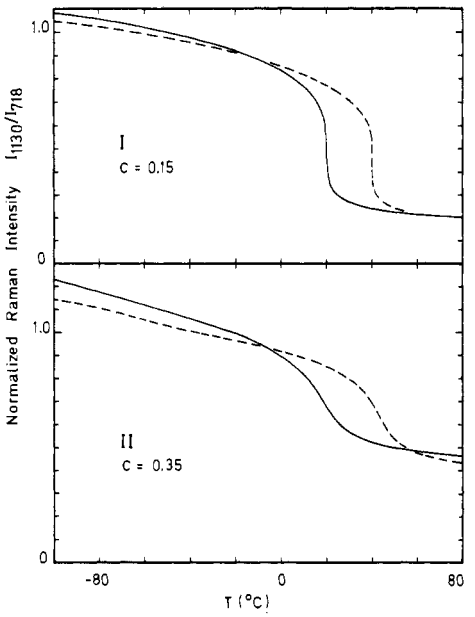

FIGURE 9: Calculated normalized Raman intensity for DMPC bilayers with cholesterol (solid curves) and DPPC bilayers with cholesterol (dashed curves) as a function of temperature. I, $c = 0.15$; II, $c = 0.35$. Note that the curves for the two phospholipids cannot be compared because a chain-length-dependent normalizing factor (see text) has not been included. The curves for each phosholipid may be compared only with the corresponding curve for $c = 0$ (Pink et al., 1980). The parameters for DMPC bilayers are those described in D. A. Pink, A. Georgallas, M. J. Zuckermann, and M. O. Steinitz (unpublished calculations): $J_0 = 0.636 \times 10^{-13}$ ergs, $J_G = 0.2$, $J_I = 0.9$, $J_E = 0.55$, $J_c = -0.866$, and $E_E = 1.94$. The remaining parameters are as given here.

for labeling the region of the phase diagram (Figure 6) as "gellike". For $c = 0.35$, however, the situation is quite different. For temperatures from $T = -60$ °C to $T = T_c$, there are between 1.5 and 3 more gauche bonds per molecule than in the pure case while there are between 1 and 4 gauche bonds less per molecule between $T = T_c$ and $T \approx 60$ °C. This is another aspect of why we have chosen to label this region of the phase diagram as intermediate.

Figure 9 shows the predicted relative intensities for a bilayer of dimyristoylphosphatidylcholine (DMPC) and cholesterol (solid lines) together with a plot of the corresponding quantity for DPPC (dashed lines). The two curves cannot be directly compared because for both phospholipids the relative intensities, $I_{1130}(0)/I_{718}(0)$ (i.e., for cholesterol concentrations $c = 0$), are both defined to be 1.0 at $T = 0$ K, and a factor involving the chain length must be included as in eq 5. Thus, the intensities plotted (as in Figures 4 and 5) are for the intensities relative to the intensity of the corresponding pure phospholipid at $T = 0$ K.

As we have pointed out, we arre not concerned with pretransitional packing effects but only with the overall change in intensity due to chain conformational changes, and we have presented a simple way of calculating these effects. Yellin & Levin (1977a) and Gaber et al. (1978) studied packing effects in pure DPPC bilayers, and the latter concluded that on being cooled through the pretransition, the hexagonal structure is distorted into a triclinic structure. Recently, Cameron et al. (1980a,b) presented evidence using infrared spectroscopy that the change in structure is from near-hexagonal to orthrhombic or monoclinic. They point out that calculations using the S_{trans} parameter, introduced by Gaber & Peticolas (1977) and used by them to interpret their Raman spectroscopy measurements, conclude that three to four gauche bonds per chain are introduced when the temperature is raised from 15 to 37 °C and

Table II: C-16 Hydrocarbon Chain State Configurations and Relative Raman Intensities. Reduced Set

state		length (C–C bond units)	degeneracy	rel Raman intensity	internal energy
all-trans	G	15	1	16.00	0
intermediate	1	14	4	7.63	E_g[a]
	2	13	4	3.13	
	3	12	4	0.63	
	4 kink	14	8	9.00	$2E_g$
	5	13	4	4.00	
	7	13	16	3.34	$3E_g$
	8	12	4	1.00	
melted	E	9	D_E	0.94	E_E

[a] E_g is the energy required to form a gauche bond, $E_g = 0.45 \times 10^{-13}$ erg (Pink et al., 1980).

that this is the same numbers of gauche bonds per chain that are introduced additionally at the main transition.

We would like to reiterate (Pink et al., 1980) that our expression for I_{1130}/I_{REF} is not in accord with S_{trans}, namely, that all-trans segments do not scatter incoherently as assumed by Gaber & Peticolas (1977) but that the scattering is due to the conformation of the entire chain. Our expression is, of course, simplified by ignoring the fact that one end of the chain is not free. From our previous calculations [Figure 7 of Pink et al. (1980)], it can be seen that at 15 °C there are about 0.75 gauche bond per chain, at 37 °C about 1.3 per chain, and just below the main transition about 1.5 gauche bonds per chain in pure DPPC. As mentioned in the introduction, these results are in agreement with the estimates of Yellin & Levin (1977b). These gauche bonds are located predominantly near the end of the lipid chain. When the bilayer melts, an additional 3.5 gauche bonds per chain are introduced, and the number of gauche bonds increases with temperature.

As a final calculation, however, we modified the model used here to recalculate relative Raman intensities for pure DPPC bilayers. Our intention was to see whether a model which assumes that only gauche conformers near the end of the hydrocarbon chain can be thermally excited below T_c will yield calculations in accord with our earlier measured relative Raman intensities. To this end, we have excluded from the states listed in Table I all those which have gauche bonds nearer to the head group than the ninth C–C bond. It will be recalled that the states of Table I exclude gauche bonds nearer to the head group than the third C–C bond. The change results in the complete exclusion of state 6 and modified degeneracies and relative Raman intensities for some of the remaining states. The states are listed in Table II. As before, we chose $E_g = 0.45 \times 10^{-13}$ ergs, but reduced the melted state energy to $E_E = 2.5 \times 10^{-13}$ ergs (5.5 gauche bonds) so that the transition would not be too hard, and adjusted its degeneracy D_E and J_0 so that a first-order transition was obtained at 41 °C with a transition enthalpy, ΔH, in accord with observation. We found that $D_E = 10^5$ and $J_0 = 0.6602 \times 10^{-13}$ ergs gave $\Delta H = 8.81$ kcal/mol. We considered that we could not make E_E any smaller since the melted bilayers have $\gtrsim 5$ gauche bonds per chain. The results are shown in Figure 10. Two points are clear. (i) The calculated relative Raman intensity does not fit as well as that calculated by using the states of Table I [Figure 5 of Pink et al. (1980)]. (ii) The average number of gauche bonds per chain are as follows: at $T = 15$ °C, ~ 0.5; at $T = 37$ °C, ~ 1; just below T_c, ~ 1.2; just above T_c, ~ 4.6. These numbers should be compared to 0.75, 1.3, 1.5, and 5 per chain as calculated by using Table

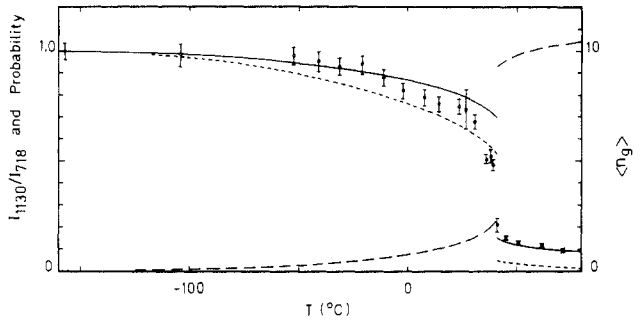

FIGURE 10: Normalized Raman intensity of pure DPPC bilayers. The calculations use the reduced set of states given in Table II (see text). The open circles are data of Pink et al. (1980). The solid line is the calculated normalized intensity, and for $T < T_c = 41$ °C, it is greater than that calculated by Pink et al. (1980) using the states of Table I. Short dashes show the probability of finding a chain in its all-trans state. Long dashes show the average number of gauche bonds per DPPC molecule, $\langle n_g \rangle$ (right-hand scale). This curve lies slightly lower than the corresponding curve [Figure 7 of Pink et al. (1980)] calculated by using the states given in Table I.

I. We can conclude, therefore, that the average number of gauche bonds per chain changes slightly but not substantially from that calculated before and that conformational changes occur predominantly in the half of the chain furthest from the head group.

There are two final points: although we are aware that Raman intensities may depend explicitly upon interchain coupling, we have not yet developed a theory of Raman intensities which depend explicitly upon the interaction between two chains.

A calculation to deduce changes in chain vibrations due to the presence of neighboring molecules would be very complicated. Our theory assumes that such direct interchain effects can be ignored without attempting to justify such an assumption. It can be mentioned, however, that recent results on crystalline n-$C_{21}H_{44}$ (R. G. Synder, D. G. Cameron, H. L. Casal, D. A. C. Compton, and H. H. Mantsch, unpublished experients) have been interpreted as indicating that the major factor involved in the decrease in intensity of the 1130-cm^{-1} band as a function of temperature is the introduction of a low population of gauche conformers. This is entirely in accord with our earlier results (Pink et al., 1980). We would argue that if interchain effects are small for a pure lipid bilayer, then they should be even smaller for that bilayer when it contains cholesterol, since cholesterol inhibits the close packing of the lipid hydrocarbon chains. Of course, the calculated average intensities depend implicitly upon chain–chain and chain–cholesterol interactions, but the relative intensities used here and previously depend explicitly only upon the internal states of the chains. It must also be remembered that we have taken the intensity of the 718-cm^{-1} band to be both temperature and concentration independent for which there is evidence. A variation of a few percent in this intensity with temperature or concentration is acceptable.

Added in Proof

Our predictions for DMPC with cholesterol concentration $c = 0$ (Pink et al. (1980; Figure 6I)) can be compared to the measurements of Susi et al. (1980) on DMPC liposomes. Note that they assume that the chains are all-trans at −50 °C. There is good agreement between these two results for $T < T_c$, but for $T > T_c$ the measured values lie above the calculated values. Recent measurements (Vogel & Jähnig, 1981) on DMPC and DPPC membranes with $c = 0$ differ from those of Susi et al. (1980) and the measurements of Pink et al. (1980). Neither Susi et al. (1980) nor Vogel & Jähnig (1981) give error bars for their measurements.

Acknowledgments

We thank David Cameron, Henry Mantsch, and Ian Smith for preprints of their papers and for useful discussions and Bruce Gaber for an informative discussion on Raman intensities. T.J.G. and D.C. thank Professor G. Wilkinson for use of the Imperial College (University of London) Raman spectroscopy facilities and B. P. O'Hare for technical assistance. We also thank an anonymous referee for some useful comments.

References

Bicknell-Brown, E., & Brown, K. G. (1980) *Biochem. Biophys. Res. Commun. 94*, 638–645.
Bunow, M. W., & Levin, I. W. (1977) *Biochim. Biophys. Acta 464*, 202–216.
Caillé, A., Pink, D. A., de Verteuil, F., & Zuckermann, M. J. (1980) *Can. J. Phys. 58*, 581–611.
Cameron, D. G., Casal, H. L., Gudgin, E. F., & Mantsch, H. H. (1980a) *Biochim. Biophys. Acta 596*, 463–467.
Cameron, D. G., Casal, H. L., & Mantsch, H. H. (1980b) *Biochemistry 19*, 3665–3672.
Estep, T. N., Mountcastle, D. B., Biltonen, R. L., & Thompson, T. E. (1978) *Biochemistry 17*, 1984–1989.
Gaber, B. P., & Peticolas, W. L. (1977) *Biochim. Biophys. Acta 465*, 260–274.
Gaber, B. P., Yager, P., & Peticolas, W. L. (1978) *Biophys. J. 21*, 161–176.
Lippert, J. L., & Peticolas, W. L. (1971) *Proc. Natl. Acad. Sci. U.S.A. 68*, 1572–1576.
Mabrey, S., Mateo, P. L., & Sturtevant, J. M. (1978) *Biochemistry 17*, 2464–2468.
Marcelja, S. (1974) *Biochim. Biophys. Acta 367*, 165–174.
Oldfield, E., & Chapman, D. (1972) *FEBS Lett. 23*, 285–297.
Pink, D. A., & Chapman, D. (1979) *Proc. Natl. Acad. Sci. U.S.A. 76*, 1542–1546.
Pink, D. A., Green, T. J., & Chapman, D. (1980) *Biochemistry 19*, 349–356.
Snyder, R. G. (1967) *J. Chem. Phys. 47*, 1316–1360.
Spiker, R. C., & Levin, I. W. (1975) *Biochim. Biophys. Acta 388*, 361–373.
Spiker, R. C., Jr., & Levin, I. W. (1976) *Biochim. Biophys. Acta 455*, 560–575.
Susi, H., Byler, D. M., & Damert, W. C. (1980) *Chem. Phys. Lipids 27*, 337–343.
Theimer, O. (1957) *J. Chem. Phys. 27*, 408–416.
Vogel, H., & Jähnig, F. (1981) *Chem. Phys. Lipids 29*, 83–101.
Wallach, D. F. H., Verma, S. P., & Fookson, J. (1979) *Biochim. Biophys. Acta 559*, 153–208.
Yellin, N., & Levin, I. W. (1977a) *Biochim. Biophys. Acta 489*, 177–190.
Yellin, N., & Levin, I. W. (1977b) *Biochemistry 16*, 642–647.